Quantitative Estimation of the Total Sulfide Concentration in Live Tissues by Two-Photon Microscopy

ARTICLE *in* ANALYTICAL CHEMISTRY · SEPTEMBER 2013

Impact Factor: 5.64 · DOI: 10.1021/ac402042k · Source: PubMed

6 AUTHORS, INCLUDING:

Lim Chang Su
Korea University
46 PUBLICATIONS **1,370** CITATIONS
SEE PROFILE

Hoon-Jai Chun
342 PUBLICATIONS **2,244** CITATIONS
SEE PROFILE

analytical chemistry

Article

pubs.acs.org/ac

Quantitative Estimation of the Total Sulfide Concentration in Live Tissues by Two-Photon Microscopy

Chang Su Lim,[†] Sajal Kumar Das,[†,§] Sun Young Yang,[†] Eun Sun Kim,[‡] Hoon Jai Chun,[‡] and Bong Rae Cho*,[†]

[†]Department of Chemistry, Korea University, 1-Anamdong, Seoul 136-701, Korea

[‡]Department of Internal Medicine, Korea University College of Medicine, 1-Anamdong, Seoul 136-705, Korea

Supporting Information

ABSTRACT: Hydrogen sulfide (H_2S) is a newly recognized transmitter, which protects various organs from oxidative stress. In this article, we report a ratiometric two-photon probe, TFCA, which can be excited by 750 nm femtosecond pulses, shows a 110-fold increase in the intensity ratio upon reaction with HS^- and high selectivity for HS^- and can visualize the total sulfide ($[H_2S] + [HS^-]$) distribution in live tissue by two-photon microscopy (TPM). We also developed a kinetic method to quantitatively estimate the total sulfide concentration ($[H_2S] + [HS^-]$) in live tissues. The kinetic method allowed us to measure the observed rate constants (k_{obs}) for the sulfide-induced deazidation reaction of TFCA in live cells and tissues using TPM. The total sulfide concentration was calculated by using $k_{obs} = k_2[HS^-]$, with the k_2 value determined in HEPES/EtOH (1/1, pH = 7.2), and $[H_2S]/[HS^-] = [H^+]/K_a$. The total sulfide concentration was found to be nearly zero in HeLa cells and 4−7 μM in rat colon tissues.

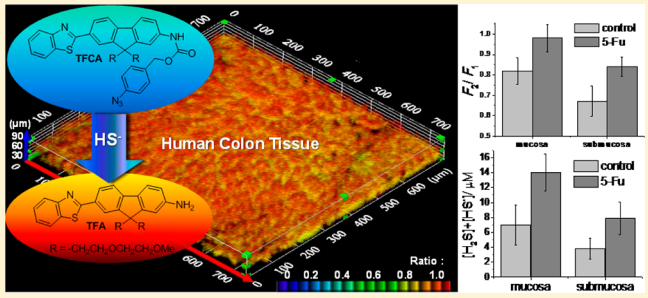

Hydrogen sulfide (H_2S), a newly recognized transmitter,[1,2] is synthesized in mammalian tissues from cysteine and homocysteine through the action of enzymes such as cystathionine β-synthase (CBS) and cystathionine γ-lyase (CSE).[3] H_2S protects gastrointestinal mucosa from injury, reduces mucosal inflammation, and augments tissue repair.[4−6] Malfunction of H_2S homeostasis has been implicated in ulcerative colitis, hypertension, atherosclerosis, cardiomyopathy, diabetic endothelial dysfunction, and diabetic nephropathy.[7−9] To elucidate its roles in biology and medicine, the detection of this small molecule in a living system is crucial.

The current methods of detecting H_2S in a living system include gas chromatography,[10,11] electrochemistry,[12−14] and colorimetry,[15−17] which require processing and/or destruction of tissues or cell lysates. Fluorescence imaging with one-photon fluorescent probes has recently emerged as a nondestructive detection method in live cells.[18−26] However, there is no reliable method to measure H_2S concentration in live tissue.

An attractive approach to the detection of H_2S in live tissue is the use of two-photon microscopy (TPM). TPM, which employs two near-infrared (NIR) photons of lower energy as the excitation source, is a new technique that can visualize biological activities deep inside intact tissues for a long period of time, when combined with an appropriate two-photon (TP) probe.[27−29] The NIR photons can penetrate deep inside tissue with minimum self-absorption and reduce tissue autofluorescence and photodamage.[27,28] Moreover, the TP excitation is intrinsically localized, thereby providing sectional imaging capability.[27,28] In this context, we developed a TP turn-on probe (FS1) that can detect HS^- in live cells and intact tissues at >100 μm depth by TPM.[29] Since H_2S and HS^- are in equilibrium, TPM images of the cells and tissues labeled with FS1 qualitatively reflected the distribution of both of the sulfide species. To quantitatively measure the total sulfide concentration ($[H_2S] + [HS^-]$) deep inside live tissues, we have now developed a ratiometric TP probe for HS^- (TFCA) (Figure 1). For reaction-based probes such as TFCA,

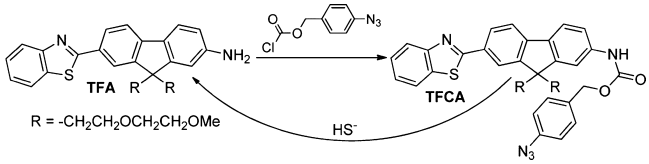

Figure 1. Structures of TFA, TFCA, and synthesis of TFCA.

however, the reaction rate is so slow that quantitative measurement of HS^- is not possible by using the probe/product ratio.[30] We, therefore, have developed a kinetic method to quantitatively estimate the total sulfide concentration with TFCA.

RESULTS AND DISCUSSION

Probe Design and Photophysical Properties. Design of a ratiometric TP probe for sulfide requires a fluorophore with

Received: July 4, 2013
Accepted: September 3, 2013
Published: September 3, 2013

Table 1. Photophysical Data for Compounds TFCA and TFA

	$\lambda^{(1)}_{max}$ (nm) (10^{-4} ε)[a]		λ^{fl}_{max} (nm)[a]		Φ[b]		$\lambda^{(2)}_{max}$ (nm)[c]		$\Phi\delta_{max}$[d] (GM)[e]	
	TFCA	TFA	TFCA	TFA	TFCA	TFA	TFCA	TFA	TFCA	TFA
EtOH	354 (4.27)	381 (4.81)	437	498	0.87	0.87				
HEPES/EtOH (1/1)	352 (4.11)	368 (4.77)	440	530	0.41	0.81	740	750	12	94
HEPES	360 (2.50)	363 (3.91)	444	548	0.013	0.46	740	750	0.67	52
cell			450	520						

[a] λ_{max} of one-photon absorption and emission spectra. [b] Fluorescence quantum yield. [c] λ_{max} of two-photon excitation spectra. [d] Estimated uncertainty, ± 15%. [e] GM = 10^{-50} cm^4 s/photon.

significant TP action cross section ($\Phi\delta_{max}$), where Φ and δ_{max} are the fluorescence quantum yield and maximum TP absorption cross section, respectively, to obtain a bright TPM image, appreciable water solubility to stain the cells, high photostability and low cytotoxicity for long-term imaging, and well-separated emission maxima of the probe before and after the reaction with HS^-. To meet such requirements, we developed TFCA by introducing an azide-based carbamate leaving group to 7-(benzo[*d*]-thiazol-2-yl)-9,9-(2-methoxyethoxy)ethyl-9*H*-fluoren-2-amine (TFA), with the anticipation that the HS^--induced deazidation followed by cleavage of the carbamate would liberate TFA, thereby red-shifting the emission maxima and increasing the TP action cross section (Figure 1). We adopted TFA as the fluorophore because it showed a significant TP action cross section with appreciable water solubility and azide as the sulfide reaction site because it exhibited high selectivity toward HS^-.[29]

TFCA and TFA showed absorption maxima (λ_{max}) at 360 nm (ε = 2.50 × 10^4 $M^{-1}\cdot cm^{-1}$) and 363 nm (ε = 3.91 × 10^4 $M^{-1}\cdot cm^{-1}$), respectively, with emission maxima (λ^{fl}_{max}) at 444 nm (Φ = 0.013) and 548 nm (Φ = 0.46), respectively, in 2-[4-(2-hydroxyethyl)piperazin-1-yl]ethanesulfonic acid (HEPES) buffer (20 mM HEPES, 100 mM KCl, pH 7.4) (Table 1). The absorption ($\Delta\lambda_{max}$ = 8 nm) and emission spectra ($\Delta\lambda^{fl}_{max}$ = 31 nm) of TFCA were relatively insensitive to the solvent polarity (Figure S1a,b), while the emission spectra of TFA showed large red shifts ($\Delta\lambda^{fl}_{max}$ = 95 nm) in the order, 1,4-dioxane < DMF < EtOH < HEPES/EtOH (1/1) < HEPES buffer (Figure S1c,d). The smaller solvatochromic effects observed for TFCA can be attributed to its smaller dipole moment. In HeLa cells, TFCA and TFA showed emission maxima at 450 and 520 nm, respectively, similar to those measured in HEPES/EtOH (1/1) (Figure 3b and Table 1). This outcome indicated that HEPES/EtOH (1/1) can adequately represent the polarity of the cellular environments.

Mechanism of Sulfide-Induced Deazidation. The reaction between TFCA and NaHS in HEPES buffer and HEPES/EtOH (1/1), monitored by LC-MS analysis, indicated TFA as the only major product (Figure S2). Also, the precipitates of sulfur or polysulfide were reported in the reaction between phenyl azide and Na_2S.[31] When 100 μM of Na_2S was added to TFCA in HEPES buffer at 37 °C, the fluorescence intensity of TFCA decreased slightly at 390−450 nm with a concomitant increase in the TFA fluorescence at 525−650 nm (Figure 2a). This process followed pseudo first-order kinetics, with k_{obs} = 2.89 × $10^{-4}\cdot s^{-1}$ (Figure 2b). Since pK_1 and pK_2 values of H_2S are 6.96 and 12.90, respectively,[32] H_2S and HS^- are the predominant sulfide species in aqueous solution regardless of whether Na_2S, NaHS, or H_2S is used as the sulfide donor. Also, since HS^- is a much better nucleophile than H_2S, HS^- should be the major reactive species under the reaction condition. Indeed, the plot of k_{obs} versus [HS^-] was a straight line passing through the origin (Figure 2c), indicating that the reaction was overall

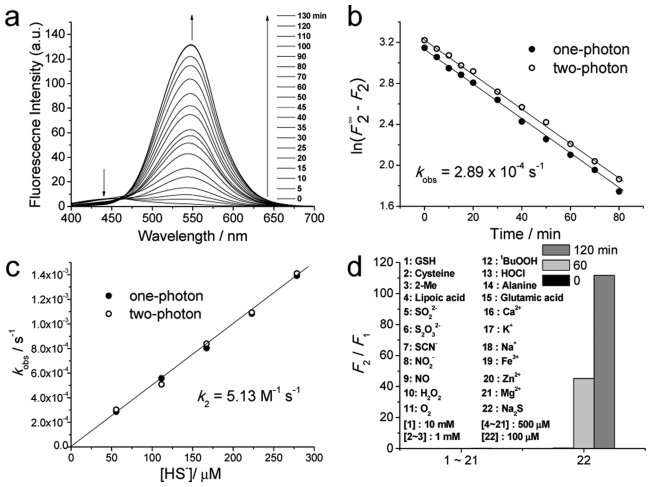

Figure 2. Spectral properties of TFCA. (a) One-photon fluorescence response with time (0−120 min) for the reactions of TFCA (5 μM) with Na_2S (100 μM). (b) Plots of ln(F^∞_2-F_2) vs time for the reactions of TFCA (5 μM) with Na_2S (100 μM) monitored by one- and two-photon processes, where F^∞_2 and F_2 are the fluorescence intensities measured after 10 half-lives and at a given time, respectively. (c) Plot of k_{obs} vs HS^- concentration. (d) Fluorescence responses of 5 μM TFCA toward 100 μM Na_2S, and other reactive sulfur, nitrogen, and oxygen species, as well as amino acids and metal ions. Bars represent the integrated fluorescence ratios (F_2/F_1) measured at the short (F_1) and long (F_2) wavelength regions at 0, 60, and 120 min. All of the data were acquired at 37 °C in HEPES buffer. The excitation wavelengths for the one- and two-photon processes were 370 and 750 nm, respectively.

second-order, first-order with respect to TFCA and first-order with respect to HS^-. The k_2 value calculated from the slope of this plot was 5.13 $M^{-1}\cdot s^{-1}$. A similar result was observed in HEPES/EtOH (1/1) (Figure S3), which is a good model for the intracellular environment (see above), except that the fluorescence intensity at 390−450 nm decreased more sharply, presumably due to the larger fluorescence quantum yield of TFCA in this solvent (Table 1). The k_2 value in HEPES/EtOH (1/1, pH = 7.2) calculated as above by using pK_a(H_2S) = 7.10 in HEPES/EtOH (1/1) was 5.17 $M^{-1}\cdot s^{-1}$, very similar to that measured in HEPES buffer. Moreover, the k_{obs} value was not influenced by the addition of *p*-dinitrobenzene (Figure S3c), a strong electron acceptor, negating the possibility of the electron transfer mechanism. These results suggest that the reaction proceeds by the rate-limiting attack of HS^- followed by the decomposition of the resulting adduct (I) as depicted in Scheme 1.

Detection of Sulfide in a TP Mode. We next evaluated the ability of TFCA to detect HS^- in a TP mode. In HEPES buffer, the TP action cross section ($\Phi\delta$) of TFCA was 0.67 GM at 740 nm, while the value for TFA was 52 GM 750 nm. In the solvent mixture of HEPES/EtOH (1/1), these $\Phi\delta$ values increased 18-fold for TFCA and approximately 2-fold for TFA (Table 1 and Figure 3a).

dx.doi.org/10.1021/ac402042k | *Anal. Chem.* 2013, 85, 9288−9295

Scheme 1. Mechanism of the Reaction between TFCA and HS^-

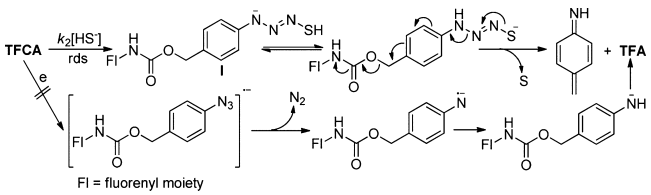

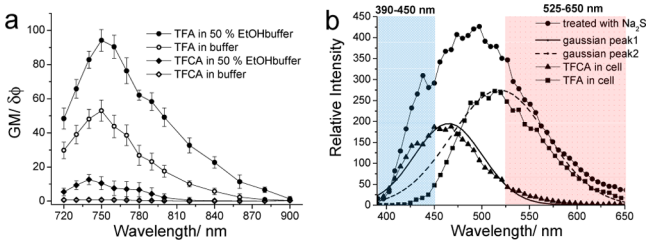

Figure 3. Two-photon excitation and fluorescence spectra of TFCA and TFA under various conditions. (a) Two-photon action spectra of TFCA and TFA (3 μM) in HEPES buffer and HEPES/EtOH (1/1). (b) Two-photon excited fluorescence (TPEF) spectra of HeLa cells labeled with TFCA or TFA. The broad curve (●) represents the TPEF spectrum of TFCA-labeled HeLa cells after treatment with 100 μM Na_2S. The solid (—) and dotted (---) lines are the dissected Gaussian functions, which are similar to the TPEF spectra of HeLa cells labeled with TFCA (▲) and TFA (■), respectively. The excitation wavelength was 750 nm.

The larger $\Phi\delta$ values measured in HEPES/EtOH (1/1) can be attributed to the larger fluorescence quantum yields (Φ) in the more hydrophobic solvent (Table 1). Moreover, the k_{obs} and k_2 values measured by the one- and two-photon processes were nearly identical (Figure 2b,c). These results allowed us to monitor the TP-excited fluorescence (TPEF) intensity of the cells and tissues that were labeled with TFCA. We then tested the utility of TFCA to detect H_2S in live cells. Using 750 nm TP excitation in a scanning lambda mode, TFCA-labeled HeLa cells treated with 100 μM Na_2S show a broad spectrum (Figure 3b), which can be dissected into two Gaussian functions with similar emission maxima and emission intensity ratios to those of TFCA and TFA measured in HEPES/EtOH (1/1), respectively. This outcome once again confirmed that HEPES/EtOH (1/1) is a good model for the intracellular environment and that TFCA can detect HS^- by TPM (see above). Moreover, the TPEF intensities of TFCA and TFA could be detected with minimum interference from each other by using the detection windows at 390−450 (1) and 525−650 nm (2), respectively. Further, the in vitro detection limit for HS^- using TFCA by TPM was found to be 0.086 μM (Figure S4).

Selectivity of TFCA for Sulfide. To test whether TFCA can selectively detect HS^- over other biologically relevant species, we determined the ratiometric responses of TFCA in the presence of various anaytes. The relative emission intensity ratio (F_2/F_1) measured at the short (F_1) and long (F_2) wavelength regions of TFCA in the presence of 100 μM Na_2S (55.7 μM HS^-) in HEPES buffer showed a 110-fold increase (Figure 2d). This outcome confirms that TFCA can serve as a ratiometric TP probe for HS^-. In contrast, TFCA exhibited no reactivity toward 10 mM glutathione (GSH, 100-fold larger amount than H_2S tested), 1 mM cysteine (Cys), and 1 mM 2-mercaptoethanol (2-ME), as well as other biologically relevant reactive sulfur species (RSS) (lipoic acid, SO_3^{2-}, $S_2O_3^{2-}$, SCN^-), reactive nitrogen species (RNS) (NO_2^-, NO), reactive oxygen species (ROS) (H_2O_2, O_2^-, *t*-BuOOH, HOCl), amino acids without thiol groups (ala, glu), and metal ions (Ca^{2+}, K^+, Na^+, Fe^{3+}, Zn^{2+}, Mg^{2+}) (Figure 2d). We note that TFCA showed small reactivity toward commercial GSH, as reported for other azide-containing probes,[18,19,24] but no reactivity toward purified GSH, as shown in Figure 2d. The negligible reactivity of GSH, Cys, and 2-ME, which cannot form an intermediate (I) with ionizable SH bond, provided additional support for the mechanism shown in Scheme 1. Moreover, TFCA and TFA were pH-insensitive in the biologically relevant pH range (Figure S5). These results established that TFCA can detect intracellular HS^- with minimum interference from other biologically relevant analytes and pH values.

Kinetic Model for the Quantitative Estimation of Sulfide. The rate equation for the reaction can be expressed as

$$-\mathrm{d}[A]/\mathrm{d}t = k_2[A][HS^-] \quad (1)$$

where [A] is TFCA concentration at time *t*.

The $[HS^-]/[H_2S]$ ratio can be expressed as

$$[HS^-]/[H_2S] = K_a/[H^+] \quad (2)$$

If $[HS^-] \gg [A]$, the integrated rate equation can be expressed as

$$-\ln[A]/[A]_0 = k_{obs}\, t \quad (3)$$

where $[A]_0$ is the TFCA concentration at $t = 0$ and $k_{obs} = k_2[HS^-]$, respectively.

Equation 3 can also be applied to live cells and tissues where H_2S homeostasis is maintained. If the H_2S concentration remains constant during the measurement, then the $[HS^-]/[H_2S]$ ratio and $[HS^-]$ should also be constant at a given pH. Under such condition, $k_{obs} = k_2[HS^-]$, and the rate equation will be identical to eq 3.

Assuming that TFCA concentration and path length are small enough so that the fluorescence intensities are proportional to [A], the fluorescence intensity in the short and long wavelength regions at a given time can be expressed as

$$F^0{}_2 = S_{A2}[A]_0 \quad (4)$$

$$F_1 = S_{A1}[A] + S_{B1}[B] \quad (5)$$

$$F_2 = S_{A2}[A] + S_{B2}[B] = S_{A2}[A] + S_{B2}([A]_0 - [A]) \quad (6)$$

$$F^\infty{}_2 = S_{B2}[A]_0 \quad (7)$$

where subscripts 1 and 2 denote short and long wavelength regions, $F^\infty{}_2$, F_1, and F_2 are the fluorescence intensities at $t = \infty$ and *t*, [B] is TFA concentration at time *t*, S_{A2}, S_{A1}, S_{B1}, and S_{B2} are the proportionality coefficients of A and B at given wavelength regions, respectively.

Solving for $[A]/[A]_0$ yields the following equations.

$$[A]/[A]_0 = (F^\infty{}_2 - F_2)/(F^\infty{}_2 - F^0{}_2) \quad (8)$$

$$-\ln(F^\infty{}_2 - F_2)/(F^\infty{}_2 - F^0{}_2) = k_{obs}\, t \quad (9)$$

Equation 9 predicts that the plot of $-\ln(F^\infty{}_2 - F_2)$ versus *t* should be linear with a slope of $-k_{obs}$. However, it is difficult to measure $F^\infty{}_2$ under imaging condition due to the deformation of the tissue samples after several hours.

Since $[A]_0 = [A] + [B]$, $F^\infty{}_1$ is negligible (Figure 3b), and the fluorescence intensities of A and B should be proportional to their concentrations, $F^\infty{}_2$ can be expressed as eq 10, if $F^0{}_1 = F^\infty{}_2$.

dx.doi.org/10.1021/ac402042k | *Anal. Chem.* 2013, 85, 9288−9295

$$F^{\infty}_2 = F_1 + F_2 \quad (10)$$

In a real system, however, $F^{0}_1 \neq F^{\infty}_2$ and eq 10 should be modified as

$$F^{\infty}_2 = (S_{B2}/S_{A1})F_1 + F_2 \quad (11)$$

F^{∞}_2 can be estimated by using eq 11. Equations 9 and 11 can also be applied to a TP process by using $F^{\infty TP}_2$, F^{TP}_2, $S_{B2}{}^{TP}$, $S_{A1}{}^{TP}$, F^{TP}_1, and F^{TP}_2 values, where superscript TP denotes the corresponding values measured in a TP mode because one- and two-photon fluorescence are essentially the same except for the excitation mode. It is worth noting that this method takes advantage of the dual channel detection capability of a ratiometric probe while avoiding the difficulty of measuring the F^{∞}_2 in the tissue samples. We then compared the F^{∞}_2 value calculated by using eq 11 with that measured in the kinetic run (Figure 2a and Figure S3a,b). The two values were identical, thereby confirming the validity of the kinetic approach.

Quantitative Estimation of the Total Sulfide Concentration in HeLa Cells. To quantitatively estimate the total sulfide concentration in live cells, we monitored the TPEF intensity of the TFCA-labeled HeLa cells in the absence and presence of Na_2S, cysteine (Cys), and glutathione (GSH) with 20−30 min intervals (Figure S6). The TPEF intensity of the TFCA-labeled HeLa cells remained nearly the same during the measurements, that is, $k_{obs} = (0.0 \pm 0.1)\ s^{-1}$. This outcome indicates that the intracellular total sulfide concentration is nearly zero, a result which concurs with others.[33] When the cells were pretreated with 100 and 300 μM Na_2S before labeling with TFCA, the TPEF intensity increased slowly with $k_{obs} = (2.6 \pm 0.9) \times 10^{-6}$ and $(7.9 \pm 1.9) \times 10^{-6}\ s^{-1}$, respectively (Figure 4).

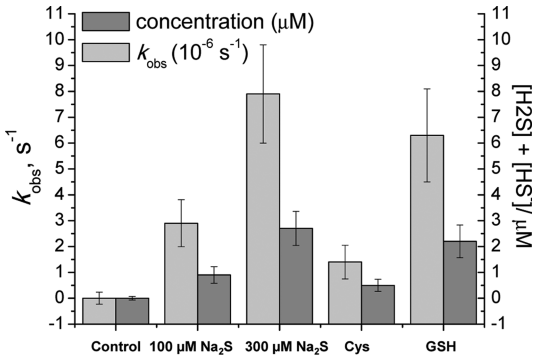

Figure 4. Average k_{obs} and sulfide concentration in HeLa cells before and after treatment with 100−300 μM Na_2S, cysteine, and glutathione estimated by the kinetic method. Error bars indicate 95% confidence intervals based on 30 k_{obs} values.

Since H_2S and HS^- are in equilibrium and $[H_2S]/[HS^-] = [H^+]/K_a = 0.794$ in HEPES/EtOH (1/1, pH = 7.2), it seems appropriate to present the total sulfide concentration ($[H_2S] + [HS^-]$). The total sulfide concentrations calculated by using $k_{obs} = k_2[HS^-]$, $k_2 = 5.17\ M^{-1}{\cdot}s^{-1}$ and $[H_2S]/[HS^-] = 0.794$ are 0.90 ± 0.32 and 2.7 ± 0.7 μM in the cells pretreated with 100 and 300 μM Na_2S, respectively. This outcome indicates that either small fraction of the H_2S penetrates the cell membrane or excess sulfide was quickly removed from the cellular environment by various degradative pathways,[1] a result in contrast to the generally accepted view that H_2S can freely penetrate the cell membrane because it is lipophilic.[39] When the cells were treated with 500 μM Cys or GSH, which are the precursors to H_2S,[34] the k_{obs} value increased from 0.0 to $(1.4 \pm 0.7) \times 10^{-6}$ to $(6.3 \pm 1.8) \times 10^{-6}\ s^{-1}$, which corresponds to an increase in the total sulfide concentration from 0.0 ± 0.1 to 0.50 ± 0.23 to 2.2 ± 0.6 μM, respectively (Figure 4). These additives seem to stimulate the cells to produce the extra sulfides,[22] but the effect appears to be modest. Further, TFCA showed negligible toxicity as measured by using a CCK-8 kit (Figure S7) and high photostability as indicated by the negligible decay in the TPEF intensity at a given spot on the TFCA-labeled HeLa cells after continuous irradiation of the fs-pulses for 60 min (Figure S8). These findings establish that TFCA can measure the total sulfide concentration in live cells by the kinetic method with minimum interference from cytotoxicity and photostability.

Quantitative Estimation of the Total Sulfide Concentration in Rat Tissue. We further investigated the utility of TFCA in a live tissue from a 5 week-old rat colon. We were particularly interested in the mucosa, muscularis mucosae, and submucosa (Figure 5c) because they are invaded in the initial stage of tumor.[35] Since it takes a longer time to stain the tissues during which time they may be deformed, excess amount (20 μM) of TFCA was used to facilitate staining. Because the structure of the colon tissue is heterogeneous, we acquired TPEF intensities from 150 sections along the z-direction at a depth of about 90−170 μm using the two detection windows (1 and 2) to visualize the overall sulfide distribution. The TPM ratiometric images constructed from F_2/F_1 revealed that the glands were clearly visible up to 146 μm depth and began to disappear as the fibres became more visible at a deeper depth (Figure 5a and Figure S9). We, therefore, divided the sections into two regions and assigned them as mucosa (90−150 μm) and submucosa including muscularis mucosae (151−170 μm), respectively. Because the mucosal layer was facing down toward the glass-bottomed dish during the experiments, it appears shallow. The TPM ratiometric images reveal that the basal sulfide level is higher in mucosa than in submucosa with the average emission ratios of 0.82 ± 0.07 and 0.67 ± 0.07, respectively (Figure 5d). The larger F_2/F_1 ratio measured in the mucosa is as expected because the mucosa is lined with columnar epithelial cells, while the submucosa is composed of connective tissue. When the rats were treated with 5-fluorouracil (5-FU), the emission ratio of the tissue slice increased slightly to 0.98 ± 0.07 in the mucosal layer and to 0.84 ± 0.05 in the submucosa. The increase in the F_2/F_1 ratio after treatment with 5-FU is consistent with the proposal that it may elevate the sulfide level by inducing mucosal inflammation (see above).[36,37] Moreover, the ratio is much smaller than $F_2/F_1 = 110$ measured in HEPES buffer after complete deazidation, a result consistent with the small sulfide concentration estimated by the kinetic method (see below). However, this ratio cannot be converted to the total sulfide concentration; that is, the ratiometric measurements can provide qualitative information, not quantitative data.

To quantitatively estimate the total sulfide concentration, we performed kinetic experiments in the colon tissues labeled with TFCA. The k_{obs} values determined in the mucosa and submucosa are $(2.0 \pm 0.8) \times 10^{-5}$ and $(1.1 \pm 0.5) \times 10^{-5}\ s^{-1}$, respectively. Upon treatment with 5-FU, these values doubled to $(4.0 \pm 0.7) \times 10^{-5}$ in the mucosa and $(2.3 \pm 0.6) \times 10^{-5}\ s^{-1}$ in the submucosa (Figure S10). The total sulfide concentration in the mucosa and submucosa reflected the same doubling trend upon 5-FU treatment, with levels of 7.0 ± 2.7 and 3.8 ± 1.4 μM before treatment and 14 ± 3 and 7.9 ± 2.2 μM, respectively, after treatment with 5-FU (Figure 5e). The higher sulfide concentration in the mucosa than in the submucosa as well as

dx.doi.org/10.1021/ac402042k | Anal. Chem. 2013, 85, 9288−9295

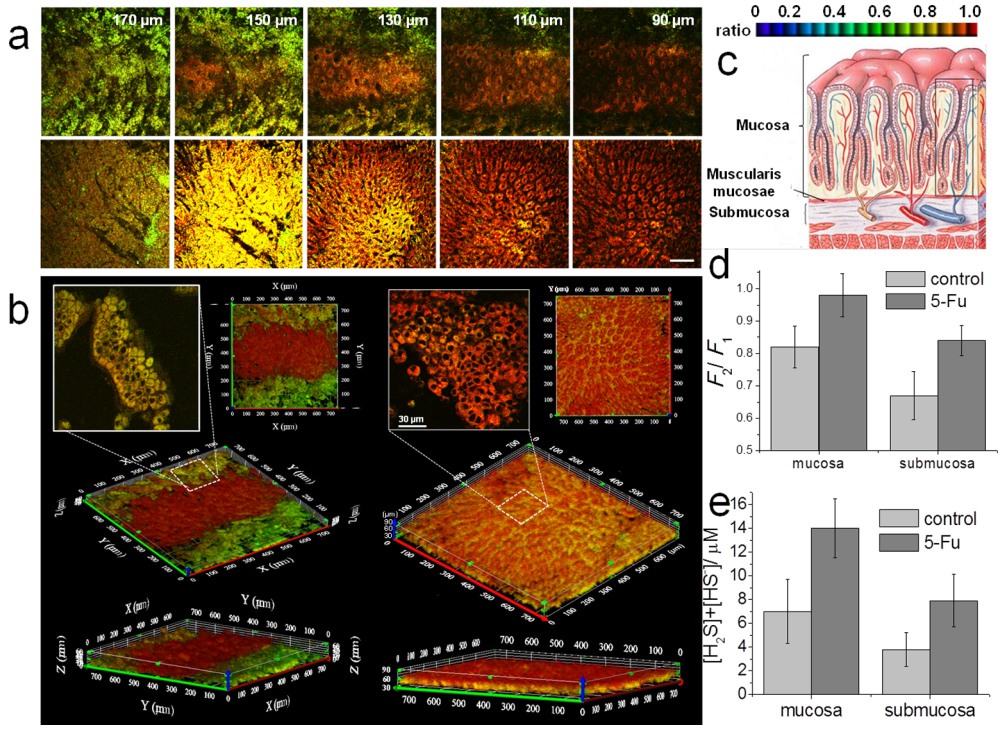

Figure 5. Pseudo-colored ratiometric TPM images of mouse colon tissues labeled with TFCA (20 μM). (a) TPM images of tissues before (upper column) and after treatment with 5-fluorouracil (bottom column) for 8 h at a depth of about 90−170 μm with magnification at 20×. Scale bar, 150 μm. (b) Three-dimensional images (top, tilted, and side views) of the colon tissues constructed from 150 TPM images obtained before (left column) and after treatment with 5-fluorouracil (right column) for 8 h at a depth of about 90−170 μm with magnification at 20×. White box shows expanded image of selected region (white-dotted box) with magnification at 100×. (c) Figure showing mucosa, muscularis mucosae, and submucosa layer taken from www.as.miami.edu. (d) F_2/F_1 ratios measured 2 h after incubation with TFCA (20 μM) in the mucosa and submucosa before and after treatment with 5-fluorouracil. Error bars indicate 95% confidence intervals based on 105 and 45 F_2/F_1 ratios measured in the mucosa and submucosa, respectively. (e) Sulfide concentration in mucosa and submucosa before and after treatment with 5-fluorouracil estimated by the kinetic method. Error bars indicate 95% confidence intervals based on 105 and 45 F_2/F_1 ratios and 112 and 48 k_{obs} values measured in the mucosa and submucosa, respectively.

the enhanced total sulfide concentration after treatment with 5-FU are in good agreement with the larger F_2/F_1 ratios measured under the same condition (see above). However, these values are much smaller than that of 50−160 μM which is measured in rat brain tissues.[40] Since too high a concentration of sulfide may alter cellular function, the smaller concentration estimated in this study seems more reasonable. Moreover, a change of the sulphide concentration in cells with mucositis may be one of the physiologic inflammation processes.[41] Further, considering that the literature method utilized processing and/or destruction of the tissue samples, our method, which takes advantage of the in vivo kinetic analysis and intact tissue imaging capabilities of TPM, should provide a more accurate estimate. These findings establish that TFCA can quantitatively estimate the total sulfide concentration in different layers of rat colon tissue within 20−40% accuracy by the kinetic method. However, the large error involved in this measurement is primarily due to the heterogeneous nature of the tissue slices taken from different rats, not due to the kinetic model presented here.

SUMMARY AND CONCLUSIONS

In this work, we synthesized a ratiometric TP probe (TFCA), which showed a 110-fold increase in the F_2/F_1 ratio upon reaction with HS^- and high selectivity for HS^-. We also developed a kinetic method by which the observed rate constants (k_{obs}) for the sulfide-induced deazidation reactions of TFCA in live cells and intact tissues could be determined. The total sulfide concentration ($[H_2S] + [HS^-]$) can then be calculated by using $k_{obs} = k_2[HS^-]$, k_2, and $[H_2S]/[HS^-] = [H^+]/K_a$. The total sulfide concentration was found to be nearly zero in the HeLa cells and 4−7 μM in rat colon tissues. Although the k_2 and $[HS^-]/[H_2S]$ values measured in HEPES/EtOH (1/1) may not be identical to the real values in the cells and tissues, the total sulfide concentration estimated by this method would provide a more quantitative insight into the physiology of the sulfide in the living system. Further, the kinetic method developed in this study will find useful applications in the quantitative estimation of biological analytes in the living system by using the reaction-based probes and TPM.

EXPERIMENTAL SECTION

Materials. Commercial L-gutathione (Aldrich, 99%) was purified by MPLC using 0.1% trifluoroacetic acid in H_2O (20 min) and 0.1% trifluoroacetic acid in MeCN (20 min) as the eluents. TFA was available from our previous work.[29] All other reagents were used as received.

Synthesis of TFCA. To a stirred solution of TFA (0.50 g, 0.96 mmol) and anhydrous Et_3N (0.28 mL, 2.0 mmol) in dry CH_2Cl_2 (15 mL) was added dropwise a solution of triphosgene (0.29 g, 0.98 mmol) in dry CH_2Cl_2 (5 mL) at −10 °C under argon atmosphere. The resulting solution was stirred for 3 h at the same temperature, and then a solution of 4-azidobenzyl alcohol[42] (0.23 g, 1.5 mmol) in dry CH_2Cl_2 (10 mL) was added dropwise. After the addition was complete, the cooling bath was removed, and the reaction mixture was stirred at rt overnight. The reaction mixture was quenched with water (30 mL) and extracted with

dx.doi.org/10.1021/ac402042k | Anal. Chem. 2013, 85, 9288−9295

CH_2Cl_2 (3 × 50 mL). The organic layer was separated, washed by water (30 mL), brine (30 mL), dried ($MgSO_4$), and filtered. Solvent was removed under reduced pressure and column chromatography (20−40% ethyl acetate in *n*-hexane) of the crude product mixture furnished compound TFCA (0.346 g, 52%) as a light yellow semisolid. ^{1}H NMR (400 MHz, $CDCl_3$): δ 8.15 (s, 1H), 8.07 (t, 2H, J = 8.0 Hz), 7.92 (d, 1H, J = 7.6 Hz), 7.70 (d, 1H, J = 8.0 Hz), 7.66 (d, 1H, J = 8.0 Hz), 7.52−7.37 (m, 5H), 7.09 (s, 1H), 7.04 (s, 2H), 5.19 (s, 2H), 3.30−3.17 (m, 14H), 2.84−2.77 (m, 4H), 2.54−2.41 (m, 4H). ^{13}C NMR (100 MHz, $CDCl_3$): δ 168.2, 154.1, 153.1, 150.9, 149.5, 142.9, 140.1, 138.1, 134.83, 134.81, 132.7, 131.9, 129.9, 127.3, 126.3, 125.0, 122.9, 121.9, 121.5, 120.9, 119.7, 119.1, 71.6, 69.8, 66.8, 66.3, 58.8, 51.5, 39.5. HRMS−FAB (m/z): $[M + H]^+$ calcd for $C_{38}H_{40}N_5O_6S$, 694.2699; found, 694.2694.

Spectroscopic Measurements. Absorption spectra were recorded on a Hewlett-Packard 8453 diode array spectrophotometer, and fluorescence spectra were obtained with Amico-Bowman series 2 luminescence spectrometer with a 1 cm standard quartz cell. The fluorescence quantum yield was determined by using Coumarin 307 and Rhodamine B as the reference by the literature method.[43] The spectral data obtained under various conditions are summarized in Figure S1 and Table 1.

Product Analysis. The reaction of TFCA (5 μM) with NaSH (300 μM) was carried out for 2 h at 37 °C in HEPES buffer (3 mL, pH = 7.2). The LC-MS traces of TFCA, TFA, and the reaction are shown below (Figure S2). The result showed that TFA is the only product.

The pK_a Value of H_2S in HEPES/EtOH (1/1, pH 7.2) at 37.0 °C. The pK_a value of H_2S in HEPES/EtOH (1/1, pH 7.2) was estimated by using following equations.

$$HS^- + H_2O \rightleftharpoons H_2S + HO^- \; K_1 = [H_2S][HO^-]/[HS^-] \tag{1a}$$

$$H_2O \rightleftharpoons H^+ + HO^- \; K_W = [H^+][HO^-] \tag{2a}$$

$$H_2S \rightleftharpoons H^+ + HS^- \; K_a = [H^+][HS^-]/[H_2S] = K_W/K_1 \tag{3a}$$

We first measured the pH of the solution containing 10.0 mM NaSH in H_2O/EtOH (1/1) at 37.0 °C with a pH meter. The pH was 9.00. The K_1 value was calculated with eq 1a by using $[HS^-]_o$ = 10.0 mM and pH 9.00. The value was 1.00 × 10^{-8} M. The pK_a value of H_2S in HEPES/EtOH (1/1, pH 7.2) was then calculated with eq 3a by using K_1 = 1.00 × 10^{-8} M and pK_w = 15.10 reported in H_2O/EtOH (1/1).[44] The calculated pK_a value was 7.10.

Kinetic Studies in Solution. Reactions of TFCA (5 μM) with Na_2S (100−500 μM) in HEPES buffer or HEPES/EtOH (1/1, pH 7.2) were followed by monitoring the increase in the fluorescence of the TFA at 525−650 nm with a luminescence spectrometer. The kinetic studies in a TP mode were conducted by the same procedure except that the TPEF was collected upon excitation at 750 nm. In all cases, the plots of $-\ln(F^\infty_2 - F_2)$ versus t were linear with excellent correlations. The k_{obs} values were obtained from the slopes of the plots. The k_2 value was obtained from the slope of the plot of k_{obs} versus $[HS^-]$. $[HS^-]$ was calculated by assuming that all of the Na_2S was converted to HS^- and H_2S, that is, $[Na_2S] = [H_2S] + [HS^-]$, and using the relationship, $[H_2S]/[HS^-] = [H^+]/K_a$ = 0.794 in HEPES/EtOH (1/1, pH = 7.2).

Measurement of Two-Photon Cross Section. The two-photon cross section (δ) was determined by using femto second (fs) fluorescence measurement technique as described.[45] TFCA and TFA were dissolved in 20 mM HEPES buffer (pH 7.2) and HEPES/EtOH (1/1) at concentrations of 3.0 × 10^{-6} M, and then the two-photon induced fluorescence intensity was measured at 740−940 nm by using Rhodamine 6G as the reference, whose two-photon property is well-characterized.[46] The intensities of the two-photon induced fluorescence spectra of the reference and sample emitted at the same excitation wavelength were determined. The TPA cross section was calculated by using $\delta = \delta_r(S_s\Phi_r\phi_r c_r)/(S_r\Phi_s\phi_s c_s)$, where the subscripts s and r stand for the sample and reference molecules. The intensity of the signal collected by a CCD detector was denoted as S. Φ is the fluorescence quantum yield. ϕ is the overall fluorescence collection efficiency of the experimental apparatus. The number density of the molecules in solution was denoted as c. δ_r is the TPA cross section of the reference molecule.

Cell Culture. HeLa human cervical carcinoma cells were obtained from American Type Culture Collection (ATCC, Manassas, VA, USA). The cells were cultured in DMEM (WelGene, Inc., Seoul, Korea) supplemented with heat-inactivated 10% FBS (WelGene), penicillin (100 units/mL), and streptomycin (100 μg/mL). All the cell lines were maintained in a humidified atmosphere of 5% CO_2 and 95% air at 37 °C. Two days before imaging, the cells were detached and were replated on glass-bottomed dishes (MatTek). For labeling, the growth medium was removed and replaced with DMEN without FBS. The cells were incubated with TFCA (2 μM) for 30 min, washed three times with DMEM without FBS, and imaged.

Cell Viability. To confirm that the tracker could not affect the viability of HeLa cells in our incubation condition, we used CCK-8 kit (Cell Counting Kit-8, Dojindo, Japan) according to the manufacture's protocol. The results are shown in Figure S7.

Two-Photon Microscopy Imaging. TPM images of TFCA-labeled cells and tissues were obtained with spectral confocal and multiphoton microscopes (Leica TCS SP2) with a 100× (NA = 1.30 OIL) and 20× (NA = 0.50 DRY) objective lens, respectively. The TPM images were obtained with a DM IRE2Microscope (Leica) by exciting the probes with a mode-locked titanium-sapphire laser source (Coherent Chameleon, 90 MHz, 200 fs) set at wavelength 750 nm and output power 1380 mW, which corresponded to approximately 2 mW average power in the focal plane. To obtain ratiometric images, internal PMTs were used to collect the signals at 390−450 and 520−650 nm regions in an 8-bit unsigned 512 × 512 pixels at 400 Hz scan speed.

Preparation, Staining, and Ratiometric Imaging of Rat Colon Slices. This protocol followed the Korean Code of Practice for the Care and Use of Animals and was approved by the Animal Ethics Committee of the Korea University Anam Hospital, Seoul, Korea. Male Sprague−Dawley rats (235−265g) were divided into two groups (5-FU and control group). In the 5-FU group, rats were treated with a 5-FU intraperitoneal injection, 150 mg/kg of body weight (SoloPak Laboratories, Franklin Park, IL). The second group, control rats, was injected with saline. Each group consisted of four rats. All rats were injected between 9:00 pm and 12 midnight, were allowed free access to food and water, and were housed in the same room with an 8 h cycle. Eight hours after peritoneal injection, all rats were sacrificed. All rats were anesthetized, and laparotomy was performed.

Slices were prepared from the colon of rats. Colon slices were cut into 2 cm long segments, were opened by longitudinal incision, and then were placed in dulbecco's phosphate buffered solution (D-PBS; 200 mM KCl, 200 mM KH_2PO_4, 8 M NaCl,

dx.doi.org/10.1021/ac402042k | Anal. Chem. 2013, 85, 9288−9295

2.16 M $Na_2HPO_4·7H_2O$). Slices were incubated with 20 μM TFCA in D-PBS bubbled with 95% O_2 and 5% CO_2 for 30−120 min at 37 °C. Slices were then washed three times with D-PBS and transferred to glass-bottomed dishes (MatTek) and observed in a spectral confocal multiphoton microscope. TPEF intensities were collected from 110 sections at the depth of 90−150 μm (mucosal layer) and from 40 sections at the depth of 151−170 μm (submucosal layer) by using the detection windows at 390−450 and 520−650 nm. The ratiometric images were constructed with the TPEF intensities collected at each section from the two detection windows. The F_2/F_1 ratios were expressed as mean ± SD. The significance level was set at $p < 0.05$.

Kinetic Measurements in Cells and Tissue Slices. Kinetic experiments in HeLa cells were performed by the same method as described above except that the TPEF intensities from TFCA-labeled HeLa cells were monitored with 20−30 min intervals upon excitation at 750 nm. The average TPEF intensities at a given time and the S_{B2}/S_{A1} ratio obtained by dividing the TPEF intensity of TFCA at 390−450 nm by that of TFA at 525−650 nm in the HeLa cell (Figure 2b) were used in the k_{obs} calculation. The rates were measured at 10 regions of interest (ROI) in three independent cell lines to obtain a total of 30 k_{obs} values. To assess the effects of Na_2S, cysteine and GSH, HeLa cells were incubated with TFCA (2 μM) and treated with Na_2S (100, 300 μM), cysteine (500 μM) and GSH (500 μM) for 30 min. Following the incubation, the cells were washed three times with DMEM without FBS, and the rates were measured.

The kinetic experiments in the rat colon tissues were performed using four colon slices from four rats. Two sets of kinetic experiments were conducted in each slice. In one set of experiment, the TPEF intensities of eight ROI's per section at depths of 90−150 μm (mucosal layer) and at depths of 151−170 μm (submucosal layer) in the TFCA-labeled colon tissues were collected at a given time and averaged. The rates were measured from seven and three sections in mucosal and submucosal layers, respectively, to obtain a total of 112 and 48 k_{obs} values in the respective layers. The rates constants were expressed as mean ± SD. The significance level was set at $p < 0.05$.

■ ASSOCIATED CONTENT

Supporting Information

Synthesis, additional methods, supplementary Scheme 1, and Figures S1−S12. This material is available free of charge via the Internet at http://pubs.acs.org.

■ AUTHOR INFORMATION

Corresponding Author

*E-mail: chobr@korea.ac.kr.

Present Address

[§]Department of Chemical sciences, Tezpur University, Napaam, Sonitpur, Assam-784 028, India.

Author Contributions

C.S.L. and S.K.D. contributed equally.

Notes

The authors declare no competing financial interest.

■ ACKNOWLEDGMENTS

This work was supported by Korea university Grant and Korea Healthcare Technology R&D Project, Ministry of Health and Welfare, Republic of Korea (A111182), and NRF Grants (No. 2012007850 and No. 20120005860).

■ REFERENCES

(1) Li, L.; Rose, P.; Moore, P. K. *Annu. Rev. Pharmacol. Toxicol.* **2011**, *51*, 169.
(2) Zabo, C. *Nat. Rev. Drug. Discov.* **2007**, *6*, 917.
(3) Yang, G. D.; Wu, L.; Jiang, B.; Yang, W.; Qi, J.; Cao, K.; Meng, Q.; Mustafa, A. K.; Mu, W.; Zhang, S.; Snyder, S. H.; Wang, R. *Science.* **2008**, *322*, 587.
(4) Li, L.; Bhatia, M.; Moore, P. K. *Curr. Opin. Pharmacol.* **2006**, *6*, 125.
(5) Mard, S. A.; Neisi, N.; Solgi, G.; Hassanpour, M.; Darbor, M.; Maleki, M. *Dig. Dis. Sci.* **2012**, *57*, 1496.
(6) Wallace, J. L.; Ferraz, J. G. P.; Muscara, M. N. *Antioxid. Redox Signaling* **2012**, *17*, 58.
(7) Li, L.; Moore, P. K. *Trends Pharmacol. Sci.* **2008**, *29*, 84.
(8) Giacco, F.; Brownlee, M. *Circ. Res.* **2010**, *107*, 1058.
(9) Szabo, C. *Antioxid. Redox. Signal.* **2012**, *17*, 68.
(10) Radford-Knoery, J.; Cutter, G. A. *Anal. Chem.* **1993**, *65*, 976.
(11) Bérubé, P. R.; Parkinson, P. D.; Hall, E. R. *J. Chromatogr., A.* **1999**, *830*, 485.
(12) Lei, W.; Dasgupta, P. K. *Anal. Chim. Acta* **1989**, *226*, 9000.
(13) Jiménez, D.; Martínez-Máñez, R.; Sancenón, F.; Ros-Lis, J. V.; Benito, A.; Soto, J. *J. Am. Chem. Soc.* **2003**, *125*, 9000.
(14) Hughes, M. N.; Centelles, M. N.; Moore, K. P. *Free Radical Biol. Med.* **2009**, *47*, 1346.
(15) Richardson, C. J.; Magee, E. A. M.; Cummings, J. H. *Clin. Chim. Acta* **2000**, *293*, 115.
(16) Searcy, D. G.; Peterson, M. A. *Anal. Biochem.* **2005**, *341*, 40.
(17) Doeller, J. E.; Isbell, T. S.; Benavides, G.; Koenitzer, J.; Patel, H.; Patel, R. P.; Lancaster, J. R., Jr.; Darley-Usmar, V. M.; Kraus, D. W. *Anal. Biochem.* **2005**, *341*, 40.
(18) Lippert, A. R.; New, E. J.; Chang, C. J. *J. Am. Chem. Soc.* **2011**, *133*, 10078.
(19) Peng, H.; Cheng, Y.; Dai, C.; King, A. L.; Predmore, B. L.; Lefer, D. J.; Wang, B. *Angew. Chem., Int. Ed.* **2011**, *50*, 9672.
(20) Sasakura, K.; Hanaoka, K.; Shibuya, N.; Mikami, Y.; Kimura, Y.; Komatsu, T.; Ueno, T.; Terai, T.; Kimura, H.; Nagano, T. *J. Am. Chem. Soc.* **2011**, *133*, 18003.
(21) Liu, C.; Peng, B.; Li, S.; Park, C. M.; Whorton, A. R.; Xian, M. *Org. Lett.* **2012**, *14*, 2184.
(22) Qian, Y.; Karpus, J.; Kabil, O.; Zhang, S. Y.; Zhu, H. L.; Banerjee, R.; Zhao, J.; He, C. *Nat. Commun.* **2011**, *90*, 35.
(23) Zhang, D.; Jin, W. *Spectrochim. Acta, A* **2012**, *90*, 35.
(24) Yu, F.; Li, P.; Song, P.; Wang, B.; Zhao, J.; Han, K. *Chem. Commun.* **2012**, *48*, 2852.
(25) Montoya, L. A.; Pluth, M. D. *Chem. Commun.* **2012**, *48*, 4767.
(26) Hou, F.; Cheng, J.; Xi, P.; Chen, F.; Huang, L.; Xie, G.; Shi, Y.; Liu, H.; Bai, D.; Zeng, Z. *Dalton Trans.* **2012**, *41*, 5799.
(27) Zipfel, W. R.; Williams, R. M.; Webb, W. W. *Nat. Biotechnol.* **2003**, *21*, 1369.
(28) Williams, R. M.; Zipfel, W. R.; Webb, W. W. *Curr. Opin. Chem. Biol.* **2001**, *5*, 603.
(29) Das, S. K.; Lim, C. S.; Yang, S. Y.; Han, J. H.; Cho, B. R. *Chem. Commun.* **2012**, *48*, 8395.
(30) George, W. G. *Handbook of Organic Chemistry*; McGraw-Hill: New York, 1987; 8−55.
(31) Belinka, B. A., Jr.; Hassner, A. *J. Org. Chem.* **1979**, *44*, 4712.
(32) Schoonen, M. A. A.; Barnes, H. L. *Geochim. Cosmochim. Acta* **1988**, *52*, 649.
(33) Furne, J.; Saeed, A.; Levitt, M. D. *Am. J. Physiol.* **2008**, *295*, 1479.
(34) Singh, S.; Padovani, D.; Leslie, R. A.; Chiku, T.; Banerjee, R. *J. Biol. Chem.* **2009**, *284*, 22457.
(35) Edge, S. B.; Compton, C. C. *AJCC Cancer Staging Manual*, 6th ed.; Springer-Verlag: New York, 2002.
(36) Jebb, S. A.; Osborne, R. J.; Maughan, T. S.; Mohideen, N.; Mack, P.; Mort, D.; Shelley, M. D.; Elia, M. *Br. J. Cancer* **1994**, *70*, 732.
(37) Wallace, J. L.; Vong, L.; McKnight, W.; Dicay, M.; Martin, G. R. *Gastroenterology* **2009**, *137*, 569.
(38) Zandarzo, R. C. O.; Brancaleone, V.; Distrutti, E.; Fiorucci, S.; Cirino, G.; Wallace, J. L. *FASEB J.* **2006**, *20*, 2118.
(39) Taniguchi, S.; Niki, I. *J. Pharmacol. Sci.* **2011**, *116*, 1.

(40) Warenycia, M. W.; Goodwin, L. R.; Benishin, C. G.; Reiffenstein, R. J.; Francom, D. M.; Taylor, J. D.; Dieken, F. P. *Biochem. Pharmacol.* **1989**, *38*, 973.
(41) Sonis, S. *J. Supportive Oncol.* **2004**, *2*, 21.
(42) Gorska, K.; Manicardi, A.; Barluenga, S.; Winssinger, N. *Chem. Commun.* **2011**, *47*, 4364.
(43) Demas, J. N.; Crosby, G. A. *J. Phys. Chem.* **1971**, *75*, 991.
(44) Karásková, E.; Mollin, J. *Chem. Pap.* **1993**, *47*, 156.
(45) Lee, K.; Yang, W. J.; Choi, J. J.; Kim, C. H.; Jeon, S. J.; Cho, B. R. *Org. Lett.* **2005**, *7*, 323.
(46) Makarov, N. S.; Drobizhev, M.; Rebane, A. *Optics Express.* **2008**, *6*, 4029.